Supersolidity of α cluster structure in ^{40}Ca

S. Ohkubo

Research Center for Nuclear Physics, Osaka University, Ibaraki, Osaka 567-0047, Japan

α cluster structure in nuclei has been long understood based on the geometrical configuration picture. By using the spatially localized Brink α cluster model in the generator coordinate method, it is shown that the α cluster structure has the apparently opposing duality of crystallinity and condensation, a property of supersolids. To study the condensation aspects of the α cluster structure a field theoretical superfluid cluster model (SCM) is introduced, in which the order parameter of condensation is incorporated by treating rigorously the Nambu-Goldstone mode due to spontaneous symmetry breaking of the global phase. The α cluster structure of ^{40}Ca, which has been understood in the crystallinity picture, is studied by the SCM with ten α clusters. It is found that the α cluster structure of ^{40}Ca is reproduced by the SCM in addition to ^{12}C reported in a previous paper, which gives support to the duality of the α cluster structure. The emergence of the mysterious 0^+ state at the lowest excitation energy near the α threshold energy is understood to be a manifestation of the Nambu-Goldstone zero mode, a soft mode, due to the condensation aspect of the duality similar to the Hoyle state in ^{12}C. The duality of α cluster structure with incompatible crystallinity and coherent wave nature due to condensation is the consequence of the Pauli principle, which causes clustering.

I. INTRODUCTION

A supersolid is a solid with superfluidity, and has been sought in recent decades in He II [1–5]. Recently it was created experimentally in an optical lattice [6–13]. The observation of the Nambu-Goldstone mode [14–16] due to spontaneous symmetry breaking (SSB) of the global phase gives direct evidence of supersolidity for an optical lattice [11–13]. Very recently the existence of supersolidity of subatomic nature—supersolidity of the three α cluster structure in the nucleus ^{12}C—was discussed [17].

The α particle model, in which the boson α particle with spin 0 is considered as a constituent unit of the nucleus, was proposed as the first nuclear structure model in 1937 [18–20] but criticized [21] in the advent of the shell model [22,23] and the collective model [24]. However, the successful shell model and the collective model [25–27] also encountered difficulty explaining the emergence of very low-lying intruder states in light nuclei such as the mysterious 0_2^+ (6.05 MeV) state in ^{16}O [28,29]. The α cluster model based on the geometrical crystallinity picture, in which the effect of the Pauli principle is taken into account, was revived and has witnessed tremendous success in recent decades in explaining both shell-model-like states and α cluster states comprehensively, which are reviewed for light nuclei in Refs. [30–32] and for the medium-weight nuclei in Refs. [33,34].

The Brink cluster model based on the geometrical crystallinity picture using the generator coordinate method (GCM) [35], the resonating group method (RGM), which is equivalent to the GCM [36], and the orthogonality condition model (OCM) [37] and the local potential model (LPM) [38–41]—both of which are approximations of the RGM and take into account of the Pauli principle by excluding the Pauli forbidden states in the RGM—have been successful in understanding the structure of nuclei [30–34]. Examples are the two α dumbbell structure of ^{8}Be [42,43], the three α triangle structure of ^{12}C [44–46], and the $\alpha + {}^{16}$O structure in ^{20}Ne [47–49]. The unified understanding of cluster structure in the low energy region, and prerainbows and nuclear rainbows in the scattering region, which are confirmed for systems such as $\alpha + {}^{16}$O and $\alpha + {}^{40}$Ca [41,50], support the geometrical crystallinity picture of the cluster structures.

Very recently Ohkubo *et al.* [17] used a field theoretical superfluid cluster model (SCM) for ^{12}C to report that the α cluster structure has a duality of crystallinity and condensation, a property of supersolidity. According to this theory, while the former is the view from the particle nature of the cluster structure, the latter is the view from the wave nature due to the coherence of the condensate cluster structure. It is important to clarify whether this supersolidity of α cluster structure is inherent only to the three α cluster structure of ^{12}C or a general property of α cluster structure with geometrical crystallinity. α cluster structure was recently paid attention from the viewpoint of quantum phase transition [51,52].

In this paper, by using the Brink α cluster model it is shown generally that α cluster structure has the duality of apparently exclusive properties of crystallinity and condensation, i.e., supersolidity. The α cluster structure of ^{40}Ca, which has been understood from the viewpoint of geometrical cluster structure, is studied from the viewpoint of condensation, superfluidity, by using a field theoretical superfluid α cluster model which rigorously treats spontaneous symmetry

breaking of the global phase due to condensation. The mechanism of why the mysterious 0^+ state in ^{40}Ca emerges as a collective state at very low excitation energy, which has been a longstanding subject in the shell model and the collective model, is investigated and is shown to arise as a member state of the Nambu-Goldstone (NG) zero mode due to global phase locking caused by the condensation aspect of the duality of α clustering in ^{40}Ca.

The organization of this paper is as follows. In Sec. II by using the Brink cluster model it is generally shown that α cluster structure has a dual property of crystallinity and condensation. In Sec. III a field theoretical superfluid cluster model with the order parameter of condensation, in which spontaneous symmetry breaking of the global phase due to condensation is rigorously treated, is given. In Sec. IV α cluster structure in ^{40}Ca is studied. First, historical attempts to understand the mysterious 0^+ state of ^{40}Ca in the shell model, collective model, and the α cluster model are briefly reviewed. It is summarized that by the observation of the $K = 0^-$ band with the α cluster structure, which was predicted from the study of anomalous large angle scattering in $\alpha + {}^{36}$Ar scattering, the geometrical α cluster model was confirmed. Second, from the viewpoint of the duality of crystallinity and condensation, the condensation aspect of the α cluster of ^{40}Ca is studied using the superfluid cluster model. The mechanism of the emergence of a mysterious 0^+ state is investigated. Sec. V is devoted to discussion. A summary is given in Sec. VI.

II. THE DUALITY OF THE α CLUSTER STRUCTURE: CRYSTALLINITY AND CONDENSATION

I show that α cluster structure with crystallinity has condensate nature simultaneously by using the Brink α cluster model based on the geometrical crystallinity picture. The n-α cluster model based on a geometrical crystalline picture, such as the two α cluster model of ^{8}Be and the three α cluster model of ^{12}C, is given by the following Brink wave function [35]:

$$\Phi_{n\alpha}^B(\boldsymbol{R}_1, \ldots, \boldsymbol{R}_n) = \frac{1}{\sqrt{(4n)!}} \det[\phi_{0s}(\boldsymbol{r}_1 - \boldsymbol{R}_1)\chi_{\tau_1, \sigma_1} \cdots$$
$$\times \phi_{0s}(\boldsymbol{r}_{4n} - \boldsymbol{R}_n)\chi_{\tau_{4n}, \sigma_{4n}}], \quad (1)$$

where $\boldsymbol{R}_i$ is a parameter that specifies the center of the ith α cluster. $\phi_{0s}(\boldsymbol{r} - \boldsymbol{R})$ is a $0s$ harmonic oscillator wave function with a size parameter b around a center $\boldsymbol{R}$,

$$\phi_{0s}(\boldsymbol{r} - \boldsymbol{R}) = \left(\frac{1}{\pi b^2}\right)^{3/4} \exp\left[-\frac{(\boldsymbol{r} - \boldsymbol{R})^2}{2b^2}\right], \quad (2)$$

and $\chi_{\tau, \sigma}$ is the spin-isospin wave function of a nucleon. Equation (1) is rewritten as

$$\Phi_{n\alpha}^B(\boldsymbol{R}_1, \ldots, \boldsymbol{R}_n) = \mathscr{A}\left[\prod_{i=1}^n \exp\left\{-2\frac{(\boldsymbol{X}_i - \boldsymbol{R}_i)^2}{b^2}\right\}\phi(\alpha_i)\right], \quad (3)$$

where $\boldsymbol{X}_i$ is the center-of-mass coordinate of the ith α cluster and $\phi(\alpha_i)$ represents the internal wave function of the ith α cluster. $\mathscr{A}$ is the antisymmetrization operator. The generator coordinate wave function $\Psi_{n\alpha}^{\text{GCM}}$ based on the geometrical

configuration of the Brink wave function is given by

$$\Psi_{n\alpha}^{\text{GCM}} = \int d^3\boldsymbol{R}_1 \cdots d^3\boldsymbol{R}_n f(\boldsymbol{R}_1, \ldots, \boldsymbol{R}_n)$$
$$\times \Phi_{n\alpha}^B(\boldsymbol{R}_1, \ldots, \boldsymbol{R}_n). \quad (4)$$

I show that the cluster model with crystallinity of Eq. (4) has the property of condensation. For the sake of simplicity I treat hereafter the simplest two α cluster structure of ^{8}Be. The generator coordinates $\boldsymbol{R}_1$ and $\boldsymbol{R}_2$, which specify the position parameters of the two α clusters, are rewritten as follows by using $\boldsymbol{R}_G$ and $\boldsymbol{R}$, which are the center-of-mass and the relative vectors, respectively:

$$\boldsymbol{R}_1 = \boldsymbol{R}_G + \tfrac{1}{2}\boldsymbol{R}, \quad \boldsymbol{R}_2 = \boldsymbol{R}_G - \tfrac{1}{2}\boldsymbol{R}. \quad (5)$$

I take $\boldsymbol{R}_G = 0$ to remove the spurious center-of-mass motion and use the notation $\Phi_{2\alpha}^B(\boldsymbol{R})$ for $\Phi_{2\alpha}^B(\frac{1}{2}\boldsymbol{R}, -\frac{1}{2}\boldsymbol{R})$. Thus Eq. (4) is written as

$$\Psi_{2\alpha}^{\text{GCM}} = \int d^3\boldsymbol{R} f(\boldsymbol{R})\Phi_{2\alpha}^B(\boldsymbol{R}). \quad (6)$$

$\Psi_{2\alpha}^{\text{GCM}}$ is obtained by solving the Hill-Wheeler equation for $f(\boldsymbol{R})$. I introduce $g(\boldsymbol{\mu})$, which is related to $f(\boldsymbol{R})$ by the Laplace transformation

$$f(\boldsymbol{R}) = \int_0^\infty d\mu_x \int_0^\infty d\mu_y \int_0^\infty d\mu_z$$
$$\times \exp\left[-\left(\mu_x R_x^2 + \mu_y R_y^2 + \mu_z R_z^2\right)\right]g(\boldsymbol{\mu}), \quad (7)$$

where $\boldsymbol{\mu} = (\mu_x, \mu_y, \mu_z)$. Then Eq. (6) reads

$$\Psi_{2\alpha}^{\text{GCM}} = \int d^3\boldsymbol{\mu} g(\boldsymbol{\mu})\left[\int d^3\boldsymbol{R} \exp\left\{-\left(\mu_x R_x^2 + \mu_y R_y^2\right.\right.\right.$$
$$\left.\left.\left. + \mu_z R_z^2\right)\right\}\Phi_{2\alpha}^B(\boldsymbol{R})\right]. \quad (8)$$

By rewriting the term $[\cdots]$ in the right-hand side of Eq. (8) as $\Phi_{2\alpha}^{\text{PCM}}(\boldsymbol{\mu})$, defined by

$$\Phi_{2\alpha}^{\text{PCM}}(\boldsymbol{\mu}) \equiv \int d^3\boldsymbol{R} \exp\left[-\left(\mu_x R_x^2 + \mu_y R_y^2\right.\right.$$
$$\left.\left. + \mu_z R_z^2\right)\right]\Phi_{2\alpha}^B(\boldsymbol{R}), \quad (9)$$

$$\propto \mathscr{A}\left[\prod_{i=1}^2 \exp\left\{-2\left(\frac{X_{ix}^2}{B_x^2} + \frac{X_{iy}^2}{B_y^2} + \frac{X_{iz}^2}{B_z^2}\right)\right\}\phi(\alpha_i)\right], \quad (10)$$

with $B_k = \sqrt{b^2 + \mu_k^{-1}}$ ($k = x, y, z$), Eq. (8) reads

$$\Psi_{2\alpha}^{\text{GCM}} = \int d^3\boldsymbol{\mu} g(\boldsymbol{\mu})\Phi_{2\alpha}^{\text{PCM}}(\boldsymbol{\mu}). \quad (11)$$

The $\Phi_{2\alpha}^{\text{PCM}}$ in Eq. (10), which is called a nonlocalized cluster model (NCM) or a THSR cluster wave function in Refs. [53,54] and suggested to be a pseudocondensate model (PCM) in Ref. [17], shows that α clusters are sitting in the $0s$ orbit of the trapping harmonic oscillator potential with an oscillator parameter $\boldsymbol{B} = (B_x, B_y, B_z)$ and represents the condensed aspect of the α clusters. This trapping harmonic oscillator potential corresponds to the trapping harmonic oscillator potential in the superfluid cluster model discussed in
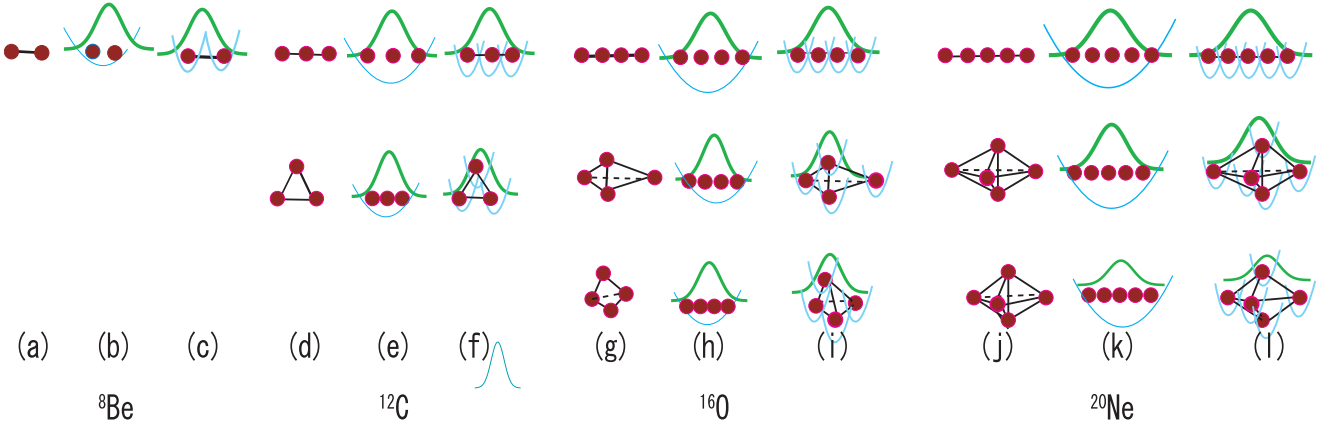
FIG. 1. Illustrative figures of crystallinity, condensation, and supersolidity of the α clusters (filled circles) proposed in ^{12}C in Ref. [17] are displayed for the simplest system ^{8}Be discussed in the text and extended to ^{16}O with four α clusters and ^{20}Ne with five α clusters. As the excitation energy increases vertically, the structure change occurs. In each nucleus crystallinity, condensation associated with a coherent wave, and supersolidity with both crystallinity and the coherent wave of the α clusters are shown. The original Ikeda diagram based on the crystallinity picture corresponds to (a), (d), (g), and (j) in each nucleus. In (b), (e), (h), and (k) of each nucleus α clusters are sitting in the 0s state of the harmonic oscillator potential with a coherent wave (broad curve). In (c), (f), (i), and (l) of each nucleus, which illustrates supersolidity, the α clusters are sitting in the 0s state of the distinct harmonic oscillator potentials separated due to the Pauli repulsion associated with a coherent wave (broad curve).

the next section, where the condensation of the trapped α clusters is rigorously treated by introducing the order parameter due to SSB of the vacuum. While in Eq. (6) the GCM wave function is expressed based on the geometrical picture using the Brink function $\Phi_{2\alpha}^B(\boldsymbol{R})$ as a base function, in Eq. (11) the same GCM wave function is expressed using the wave function $\Phi_{2\alpha}^{\text{PCM}}(\boldsymbol{\mu})$ as a base function. From Eqs. (6) and (11), it is found that the Brink α cluster model in the generator coordinate method has both the crystallinity and the condensate nature simultaneously.

The above discussion for the simplest two α cluster system can be generalized to the n-α cluster system. The Laplace transformation relation is generalized to

$$f(\boldsymbol{R}_1, \ldots, \boldsymbol{R}_n) = \int_0^\infty d\boldsymbol{\mu} \exp\left[- \sum_{i=1}^n \left(\mu_x R_{ix}^2 + \mu_y R_{iy}^2 \right. \right.$$
$$\left. \left. + \mu_z R_{iz}^2 \right) \right] g(\boldsymbol{\mu}). \tag{12}$$

Equation (9) generalized to n-α clusters is given by

$$\Phi_{n\alpha}^{\text{PCM}}(\boldsymbol{\mu}) = \int d^3\boldsymbol{R}_1 \cdots d^3\boldsymbol{R}_n \exp\left[- \sum_{i=1}^n \left(\mu_x R_{ix}^2 \right. \right.$$
$$\left. \left. + \mu_y R_{iy}^2 + \mu_z R_{iz}^2 \right) \right] \Phi_{n\alpha}^B(\boldsymbol{R}_1, \ldots, \boldsymbol{R}_n), \tag{13}$$

$$\propto \mathscr{A}\left[\prod_{i=1}^n \exp\left\{ -2\left(\frac{X_{ix}^2}{B_x^2} + \frac{X_{iy}^2}{B_y^2} + \frac{X_{iz}^2}{B_z^2} \right) \right\} \phi(\alpha_i) \right]. \tag{14}$$

Similarly to Eq. (11), one gets

$$\Psi_{n\alpha}^{\text{GCM}} = \int d^3\boldsymbol{\mu}\, g(\boldsymbol{\mu}) \Phi_{n\alpha}^{\text{PCM}}(\boldsymbol{\mu}). \tag{15}$$

Thus from Eqs. (4) and (15) it is found generally that the n-α cluster wave function in the geometrical cluster model picture has the property of condensation. This shows generally that the GCM n-α cluster wave function has the duality of crystallinity and condensation independently of the Hamiltonian used.

Illustrative pictures based on the above geometrical structure and the condensate structure of the α clusters in ^{8}Be, ^{12}C, ^{16}O, and ^{20}Ne are displayed in Fig. 1. The pictures (a), (d), (g), and (j) correspond to the Ikeda diagram [47,55] based on the crystallinity. The pictures (b), (e), (h), and (k) represent the wave aspect of the α cluster structure due to the condensation. The two exclusive pictures, the duality of crystallinity and a condensate coherent wave, can be unified in the pictures displayed in (c), (f), (i), and (l) of each nucleus in Fig. 1 where the α clusters sitting in the 0s state of the distinct potentials due to the Pauli repulsion between the α clusters [56] form a coherent wave.

The de Broglie wavelength of each 0s state α cluster with very low energy is far longer than the geometrical distance between the α clusters. In other word, the phases of the waves are locked to form a coherent wave function, i.e., superfluidity (condensation) of the system. This is general and independent of the geometrical configuration and number of the α clusters involved, n. Therefore in principle, whatever the geometrical configuration is—triangle ($n = 3$) structure of ^{12}C, tetrahedron ($n = 4$) structure of ^{16}O [57–61], trigonal bipyramid ($n = 5$) structure of ^{20}Ne [62–66], linear chain n-α cluster ($n = 2, 3, 4, \ldots$), etc.—the geometrical α cluster structures have the potential to form a coherent wave function (superfluidity). Whether the state is superfluid depends on the superfluid density ρ_s, which encapsulates the structure and degree of clustering. The previous study of ^{12}C [17] finds that the superfluid ground state is stable with a condensation

rate 5%, giving energy levels similar to the GCM, RGM, and experiment.

III. FIELD THEORETICAL SUPERFLUID CLUSTER MODEL FOR CONDENSATION OF α CLUSTERS

The traditional cluster models involve no order parameter that characterizes condensation. A theory with no order parameter is unable to conclude whether a system under investigation is condensate or not. In Eqs. (15) and (4) no order parameter to characterize the condensation is involved. In Eq. (4) the parameter $\boldsymbol{R}$ is the order parameter to characterize the geometrical clustering. In fact, $\boldsymbol{R} = 0$ corresponds to the shell model with no clustering and $\boldsymbol{R} \neq 0$ represents the degree of geometrical clustering. On the other hand, in Eq. (15) the parameter $\boldsymbol{B}$ is not self-evidently the order parameter of condensation because global phase locking caused by spontaneous symmetry breaking due to condensation is not explicitly involved. In fact, $\boldsymbol{B} = 0$ has no physical meaning and $\boldsymbol{B} \neq 0$ does not necessarily mean condensation in Eq. (15). To conclude whether the α cluster structure has Bose-Einstein condensate (BEC) nature, it is necessary to use a theory in which the order parameter to characterize condensation is implemented.

I briefly present the formulation of the field theoretical superfluid cluster model developed in [67–69] to study BEC of α clusters in the Hoyle state and the excited states above it in ^{12}C. The model Hamiltonian for a bosonic field $\hat{\psi}(x)$ [$x = (x, t)$] representing the α cluster is given as follows:

$$\hat{H} = \int d^3x \, \hat{\psi}^\dagger(x) \left(-\frac{\nabla^2}{2m} + V_{\mathrm{ex}}(\boldsymbol{x}) - \mu \right) \hat{\psi}(x)$$
$$+ \frac{1}{2} \int d^3x \, d^3x' \, \hat{\psi}^\dagger(x) \hat{\psi}^\dagger(x') U(|\boldsymbol{x} - \boldsymbol{x}'|) \hat{\psi}(x') \hat{\psi}(x). \tag{16}$$

Here, the potential V_{ex} is a mean field potential introduced phenomenologically to trap the α clusters inside the nucleus, and is taken to have a harmonic oscillator form, $V_{\mathrm{ex}}(r) = m\Omega^2 r^2/2$. $U(|\boldsymbol{x} - \boldsymbol{x}'|)$ is the residual α–α interaction. I set $\hbar = c = 1$ throughout this paper.

When BEC of α clusters occurs, i.e., the global phase symmetry of $\hat{\psi}$ is spontaneously broken, I decompose $\hat{\psi}$ as $\hat{\psi}(x) = \xi(r) + \hat{\varphi}(x)$, where the c number $\xi(r) = \langle 0|\hat{\psi}(x)|0\rangle$ is an order parameter and is assumed to be real and isotropic. To obtain the excitation spectrum, one needs to solve three coupled equations, which are the Gross-Pitaevskii (GP) equation, Bogoliubov–de Gennes (BdG) equation, and the zero-mode equation [67,69]. The GP equation determines the order parameter by

$$\left\{ -\frac{\nabla^2}{2m} + V_{\mathrm{ex}}(r) - \mu + V_H(r) \right\} \xi(r) = 0, \tag{17}$$

where $V_H(r) = \int d^3x' \, U(|\boldsymbol{x} - \boldsymbol{x}'|)\xi^2(r')$. The order parameter ξ is normalized with the condensed particle number N_0 as

$$\int d^3x \, |\xi(r)|^2 = N_0. \tag{18}$$

The BdG equation describes the collective oscillations on the condensate by

$$\int d^3x' \begin{pmatrix} \mathcal{L} & \mathcal{M} \\ -\mathcal{M}^* & -\mathcal{L}^* \end{pmatrix} \begin{pmatrix} u_n \\ v_n \end{pmatrix} = \omega_n \begin{pmatrix} u_n \\ v_n \end{pmatrix}, \tag{19}$$

where

$$\mathcal{M}(\boldsymbol{x}, \boldsymbol{x}') = U(|\boldsymbol{x} - \boldsymbol{x}'|)\xi(r)\xi(r'),$$
$$\mathcal{L}(\boldsymbol{x}, \boldsymbol{x}') = \delta(\boldsymbol{x} - \boldsymbol{x}') \left\{ -\frac{\nabla^2}{2m} + V_{\mathrm{ex}}(r) - \mu + V_H(r) \right\}$$
$$+ \mathcal{M}(\boldsymbol{x}, \boldsymbol{x}'). \tag{20}$$

The index $\boldsymbol{n} = (n, \ell, m)$ stands for the main, azimuthal, and magnetic quantum numbers. The eigenvalue ω_n is the excitation energy of the Bogoliubov mode. For isotropic ξ, the BdG eigenfunctions can be taken to have separable forms,

$$u_n(\boldsymbol{x}) = \mathcal{U}_{n\ell}(r) Y_{\ell m}(\theta, \phi),$$
$$v_n(\boldsymbol{x}) = \mathcal{V}_{n\ell}(r) Y_{\ell m}(\theta, \phi). \tag{21}$$

One necessarily has an eigenfunction belonging to zero eigenvalue, explicitly $(\xi(r), -\xi(r))^t$, and its adjoint function $(\eta(r), \eta(r))^t$ is obtained as

$$\eta(r) = \frac{\partial}{\partial N_0}\xi(r). \tag{22}$$

The field operator is expanded as

$$\hat{\varphi}(x) = -i\hat{Q}(t)\xi(r) + \hat{P}(t)\eta(r) + \sum_n \{\hat{a} u_n(\boldsymbol{x}) + \hat{a}^\dagger v_n^*(\boldsymbol{x})\}, \tag{23}$$

with the commutation relations $[\hat{Q}, \hat{P}] = i$ and $[\hat{a}_n, \hat{a}_{n'}^\dagger] = \delta_{nn'}$. The operator $\hat{a}_n$ is an annihilation operator of the Bogoliubov mode, and the pair of canonical operators $\hat{Q}$ and $\hat{P}$ originate from the SSB of the global phase and are called the NG or zero-mode operators.

The treatment of the zero-mode operators is a chief feature of the present approach. The naive choice of the unperturbed bilinear Hamiltonian with respect to $\hat{Q}$ and $\hat{P}$ fails due to their large quantum fluctuations. Instead, all the terms consisting only of $\hat{Q}$ and $\hat{P}$ in the total Hamiltonian are gathered to construct the unperturbed nonlinear Hamiltonian of $\hat{Q}$ and $\hat{P}$, denoted by $\hat{H}_u^{QP}$ with

$$\hat{H}_u^{QP} = -(\delta\mu + 2C_{2002} + 2C_{1111})\hat{P} + \frac{I - 4C_{1102}}{2}\hat{P}^2$$
$$+ 2C_{2011}\hat{Q}\hat{P}\hat{Q} + 2C_{1102}\hat{P}^3 + \frac{1}{2}C_{2020}\hat{Q}^4$$
$$- 2C_{2011}\hat{Q}^2 + C_{2002}\hat{Q}\hat{P}^2\hat{Q} + \frac{1}{2}C_{0202}\hat{P}^4, \tag{24}$$

where

$$C_{iji'j'} = \int d^3x \, d^3x' \, U(|\boldsymbol{x} - \boldsymbol{x}'|)\{\xi(\boldsymbol{x})\}^i \{\eta(\boldsymbol{x})\}^j$$
$$\times \{\xi(\boldsymbol{x}')\}^{i'} \{\eta(\boldsymbol{x}')\}^{j'}, \tag{25}$$

and $\delta\mu$ is a counterterm that the criterion $\langle 0|\hat{\psi}|0\rangle = \xi$ determines. I set up the eigenequation for $\hat{H}_u^{QP}$, called the

zero-mode equation,

$$\hat{H}_u^{QP}|\Psi_\nu\rangle = E_\nu|\Psi_\nu\rangle \qquad (\nu = 0, 1, \dots). \qquad (26)$$

This equation is similar to a one-dimensional Schrödinger equation for a bound problem.

The total unperturbed Hamiltonian $\hat{H}_u$ is $\hat{H}_u = \hat{H}_u^{QP} + \sum_n \omega_n \hat{a}_n^\dagger \hat{a}_n$. The ground state energy is set to zero, $E_0 = 0$. The states that I consider are $|\Psi_\nu\rangle|0\rangle_{ex}$ with energy E_ν, called the zero-mode state, and $|\Psi_0\rangle \hat{a}_n^\dagger |0\rangle_{ex}$ with energy ω_n, called the BdG state, where $\hat{a}_n |0\rangle_{ex} = 0$.

IV. α CLUSTER STRUCTURE IN ^{40}Ca

In order to discuss the macroscopic concept of condensation in nuclei, it seems suitable to study a nucleus which involves many α clusters. I take ^{40}Ca with ten α clusters. In this section I apply the field theoretical superfluid cluster model to α cluster structure study of ^{40}Ca with the mysterious 0^+ state at 3.35 MeV.

First, I review briefly how the mysterious 0^+ state in the doubly magic nucleus has been understood from the viewpoint of mean field theory, i.e., the shell model and the collective model, in recent decades and how the α cluster model based on the crystallinity picture has explained the mysterious 0^+ state. Second, I study whether the α cluster states explained in the geometrical configuration picture can be understood in the viewpoint of condensation of the duality by using the SCM.

A. The mysterious 0^+ state and geometrical α cluster structure of ^{40}Ca

The emergence of the 0_2^+ at the very low excitation energy 3.35 MeV of the doubly shell-closed magic nucleus ^{40}Ca as well as the 0_2^+ state at 6.05 MeV in ^{16}O had been mysterious from the viewpoint of the shell model [28,70–72]. Brown and Green [70] pointed out the importance of deformed four-particle four-hole (4p-4h) excitations in lowering the excitation energy of the 0_2^+ state in ^{16}O. Gerace and Green [71] showed that the same situation occurs for the 0_2^+ state in ^{40}Ca. Gerace and Green [72] showed that 8p-8h excitation is important in understanding the third 0_3^+ state at 5.21 MeV. In the shell model calculations in which the ^{32}S core is assumed, Sakakura et al. [73] argued that the 0_2^+ and 0_3^+ states are dominated by the 4p-4h excitations and the 0_4^+ state at 7.30 MeV is dominated by the 8p-8h excitation.

These studies show that the vacuum ground state of ^{40}Ca is not a simple 0p-0h spherical shell model state but involves a non-negligible amount of 4p-4h correlations. To understand the excited structure is to reveal the correlations, the predisposition, of the vacuum ground state. From this viewpoint Marumori and Suzuki [29] suggested to understand the mechanism of the emergence of the mysterious 0^+ state as a collective state by defining a vacuum with correlations of the 4p-4h mode. Following this idea, the four-particle and four-hole mode-mode coupling was investigated in ^{16}O [74] and ^{40}Ca [75].

The nuclear energy density functional (EDF) approach has been applied to describe the ground state properties and the collective excitations including clustering, especially the microscopic analysis of the formation and evolution of the cluster structure from the vacuum ground state. The authors of Ref. [76] consider that cluster structures can be a transitional phase between the quantum liquid phase and the crystal phase. It is very interesting to know whether the mysterious 0^+ states in ^{40}Ca as well as in ^{16}O are reproduced in the EDF and how its mechanism of low excitation energy is understood from the viewpoint of the mean field. However, the structures of the excited energy levels in ^{40}Ca as well as ^{16}O have not been reported yet.

Also ab initio approaches, such as fermionic molecular dynamics (FMD) [77] used for ^{12}C and antisymmetric molecular dynamics (AMD) [78] used for ^{42}Ca, have not been applied to explain the mysterious 0^+ state of ^{40}Ca. In ^{16}O ab initio calculations have been unable to explain the very low excitation energy of the mysterious 0^+ state providing an excitation energy 13.3 MeV in Ref. [79] and 19.8 MeV in Ref. [80], which are two or three times larger than the experimental value, 6.05 MeV.

From the viewpoint of α cluster structure, Ogawa, Suzuki, and Ikeda [81] investigated the structure of ^{40}Ca using the $\alpha + {}^{36}$Ar cluster model, in which no $K = 0^-$ band, which is a parity-doublet partner of the $K = 0^+$ band built on the mysterious 0_2^+ state, was obtained. Since this situation looked very different from ^{16}O where the well-developed α cluster $K = 0^-$ band appears, which is a parity doublet partner of the $K = 0^+$ band built on the mysterious 0_2^+ (6.05 MeV) state [82,83], Fujiwara et al. [49] discussed that the $K = 0^+$ band in ^{40}Ca has rather strong shell model aspects than the α cluster structure.

On the other hand, from the viewpoint of unification of cluster structure in the bound and quasibound states and backward angle anomaly (BAA) or anomalous large angle scattering (ALAS) in $\alpha + {}^{36}$Ar scattering, Ohkubo and Umehara [84] showed that the 2^+ (3.90 MeV), 4^+ (5.28 MeV), and 6^+ (6.93 MeV) states built on the mysterious 0_2^+ state form a $K = 0^+$ band with the $\alpha + {}^{36}$Ar cluster structure and predicted the existence of a parity-doublet partner $K = 0^-$ band with the well-developed α cluster structure at slightly above the α threshold energy. The observation of the predicted α cluster $K = 0^-$ band by Yamaya et al. [85–87] in an α transfer reaction experiment showed that the $K = 0^-$ band and the $K = 0^+$ band have the α cluster structure. The α spectroscopic factor, $S_\alpha^2 = 0.30$, extracted from α transfer reactions [85–87] shows that the ground state has a significant α cluster correlation. The α cluster structure of ^{40}Ca was further confirmed theoretically by semimicroscopic α cluster model calculations using the orthogonality condition model by Sakuda and Ohkubo [88,89], in which not only the α cluster model space but also the shell model space are incorporated. In the OCM calculations not only the α cluster states but also the shell-model-like states in ^{40}Ca are reproduced in the $\alpha + {}^{36}$Ar cluster model.

Thus the mysterious 0^+ state of ^{40}Ca was found to emerge from the ground state with the predisposition of α clustering. The finding that the vacuum ground state involves α cluster correlations is consistent with the shell model studies in Refs. [28,70–72] and the collective model viewpoint
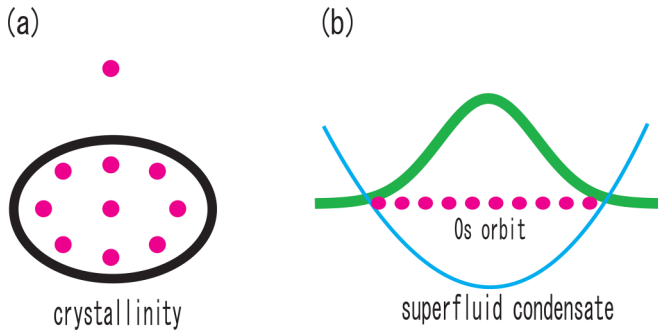
FIG. 2. Illustrative pictures of ten α clusters (filled red circles) in ^{40}Ca. (a) The crystallinity picture of the α cluster structure of ^{40}Ca with the $\alpha + {}^{36}$Ar geometrical configuration. (b) The condensation picture of the α cluster structure of ^{40}Ca in the superfluid cluster model where the ten α clusters associated a coherent wave (broad curve) are trapped in the $0s$ orbit of the confining potential.

in Refs. [29,75], which suggests that the ground state involves multiparticle-multihole, dominantly 4p-4h, shell model components. The geometrical α cluster model has been also successful in describing well the α cluster structure in the ^{40}Ca $- {}^{44}$Ti region [34,50,89].

Recently Manton [90] reported that the energy levels of ^{40}Ca can be classified as the vibration and rotation of the ten α clusters using a Skyrme model. Microscopic ten α cluster model calculations using the RGM and the GCM as well as the semimicroscopic OCM may be desired; however, such ten-body calculations are far beyond the power of the modern supercomputers. From the microscopic cluster model point of view the $\alpha + {}^{36}$Ar cluster model is an approximation of the ten α cluster model with $\boldsymbol{R}_1 = \boldsymbol{R}_2 = \cdots = \boldsymbol{R}_9$ in Eq. (4), as illustrated as in Fig. 2.

Since the crystallinity picture of the α cluster structure in ^{40}Ca has been confirmed theoretically and experimentally, the problem is to reveal the origin and the collective nature of the mysterious 0^+ state as well as the excited α cluster states from the condensation viewpoint of the duality.

B. Superfluid cluster model study of ^{40}Ca

Because the α cluster structure invokes the duality of geometrical structure and condensation as discussed in Sec. II, it is expected that the α cluster states in ^{40}Ca can be also understood from the condensation viewpoint using the SCM with the order parameter of condensation. In a previous paper [17] the SCM was applied to understand the duality of the α cluster structure of ^{12}C, for which the α cluster condensation of the Hoyle state had been thoroughly investigated theoretically and experimentally. In contrast to the computational difficulties of the ten α cluster GCM calculations, the SCM calculation is tractable for many α cluster systems. In fact, the SCM has been successfully applied to study the BEC of α clusters at high excitation energies in many nuclei, ^{12}C, ^{16}O, ^{20}Ne, etc., and in ^{48}Cr and ^{52}Fe with thirteen α clusters [69].

As in Refs. [17,67–69,91], I take the Ali-Bodmer type two-range Gaussian nuclear potential $U(|\boldsymbol{x} - \boldsymbol{x}'|) = V_r e^{-\mu_r^2 |\boldsymbol{x} - \boldsymbol{x}'|^2} - V_a e^{-\mu_a^2 |\boldsymbol{x} - \boldsymbol{x}'|^2}$, with V_r and V_a being the strength
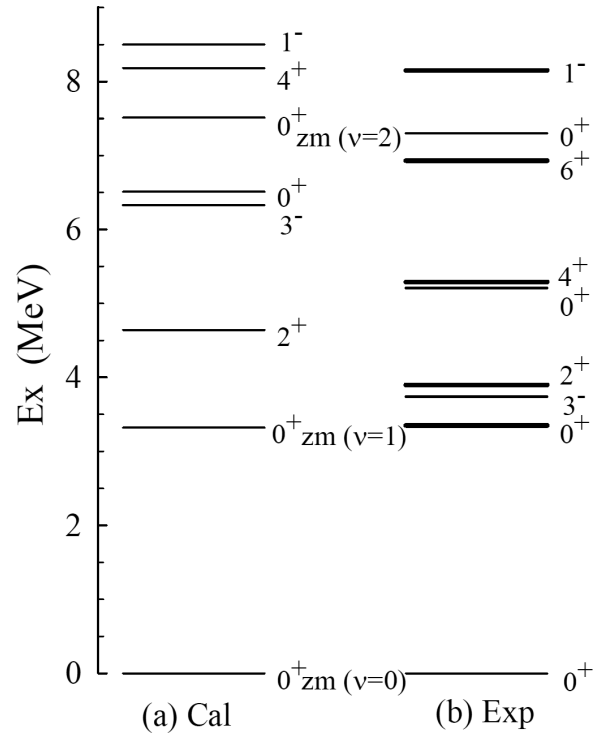

FIG. 3. (a) The energy levels of ^{40}Ca calculated with the superfluid cluster model with the condensation rate 6%. The zero-mode states are indicated by zm and others are BdG states. (b) The experimental low-lying energy levels of ^{40}Ca [86,87,93]. The member states of the experimental $K = 0^+$ and $K = 0^-$ bands with the α cluster structure are indicated by the thick solid lines.

parameters of the short-range repulsive potential due to the Pauli principle and the long-range attractive potential, respectively [92]. The chemical potential is fixed by the specification of the superfluid particle number N_0. I assume the condensation rate to be 6%, $N_0 = 0.06N$. The ground state is identified as the vacuum $|\Psi_0\rangle|0\rangle_{\rm ex}$. The range parameters μ_a and μ_r are fixed to the values 0.475 and 0.7 fm^{-1}, respectively, determined in Ref. [92] to reproduce $\alpha + \alpha$ scattering. The two potential parameters, Ω, which controls the size of the system, and V_r, which prevents collapse of the condensate, are determined to be $\Omega = 2.97$ MeV$/\hbar$ and $V_r = 591$ MeV. These reproduce the experimental root mean square (rms) radius 3.43 fm of the ground state, $|\Psi_0\rangle|0\rangle_{\rm ex}$ and the energy level of the 0_2^+ state identified as the first excited zero-mode state $|\Psi_1\rangle|0\rangle_{\rm ex}$.

In Fig. 3, the calculated energy levels are compared with the experimental data. The calculation locates the $K = 0^+$ band states in correspondence to the experimental band build on the mysterious 0_2^+ state. The moment of inertia of the calculated band is smaller than the experimental one and the 6^+ state appears at 12.75 MeV. However, it is to be noted that the α cluster band emerges at very low excitation energy from the spherical vacuum. The 0_2^+ state is a state of the Nambu-Goldstone zero mode, a soft mode collective state. This soft mode nature explains naturally why the mysterious collective 0^+ state emerges at such a low excitation energy, although it is mysteriously low for a 4p-4h state in the shell model to
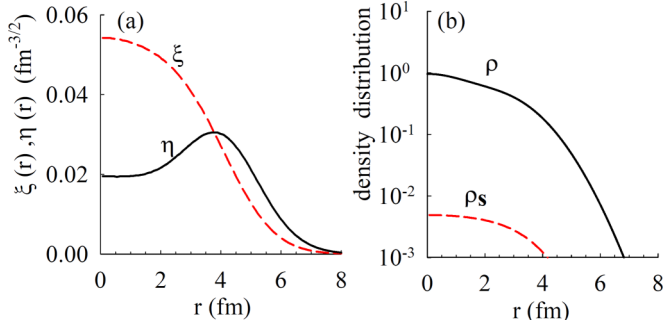
FIG. 4. (a) The calculated eigenfunction (order parameter) $\xi(r)$ (dashed line) and its adjoint eigenfunction $\eta(r)$ (solid line) for the ground state of ^{40}Ca. (b) The calculated superfluid density distribution ρ_s in the SCM (dashed line) and the matter density distribution ρ in the OCM of Ref. [88] (solid line) for the ground state.

FIG. 5. Calculated BdG wave functions of ^{40}Ca, $\mathcal{U}_{n\ell}(r)$ (solid lines) and $\mathcal{V}_{n\ell}(r)$ (dashed lines), for the 2^+ ($n=0$, $\ell=2$) and 3^- ($n=0$, $\ell=3$) states.

emerge from the spherical vacuum ground state of ^{40}Ca. If the system is infinitely large, it would appear at zero excitation energy. The finite low excitation energy is the consequence of the finite size of the nucleus and the Pauli principle. The excited states 2^+ and 4^+ of the $K=0^+$ band are the BdG states built on the NG mode state.

The calculated 0_3^+ state, which is a BdG mode state, corresponds to the experimental 0_3^+ state at 5.21 MeV above the α threshold energy, which is considered to be an 8p-8h state in the deformed model [72] and a 4p-4h dominant state in the ^{32}S core shell model calculations [73]. The calculated 0_4^+ state, which is a second member state of the NG zero mode, corresponds to the experimental 0_4^+ state at 7.30 MeV, which is interpreted to be a 4p-4h and 8p-8h dominant state in the shell model calculation [73] and a 2p-2h dominant state in the deformed model [72]. As for the negative state, a collective 3^- state appears in accordance with experiment although the calculated energy is slightly high. The 1^- state also appears to be in good correspondence with the experimental energy level, which is considered to be a band head state of the parity doublet $K=0^-$ band. It is to be noted that, although no geometrical configuration of the ten α clusters are assumed, the important α cluster states are obtained in good accordance with experiment by the SCM calculation based on the picture of Fig. 2.

In Fig. 4(a) the calculated eigenfunction $\xi(r)$ (the order parameter) and its adjoint eigenfunction $\eta(r)$ are displayed. The number fluctuation of the superfluid α clusters in the ground state, η, is large near the surface region and decreases toward the inner and outer regions. In Fig. 4(b) $\rho_s(r) = |\xi(r)|^2/N_0$ represents the calculated superfluid density distribution of the α clusters and $\rho(r)$ is the nuclear matter density distribution calculated in the OCM cluster model of Refs. [88]. ρ_s is largest in the center of the nucleus and gradually decreases toward the surface region. The nonsuperfluid normal density, $\rho_n \equiv \rho - \rho_s$, is much smaller than ρ. However, it is this small superfluid density component that causes the 0_2^+ state at such low excitation energy as an NG zero-mode state. This may evoke that the Cooper pairs, a small fraction of nucleons near the Fermi surface, cause the superfluidity of nuclei in the heavy mass region. The superfluid fraction ρ_s in the ground
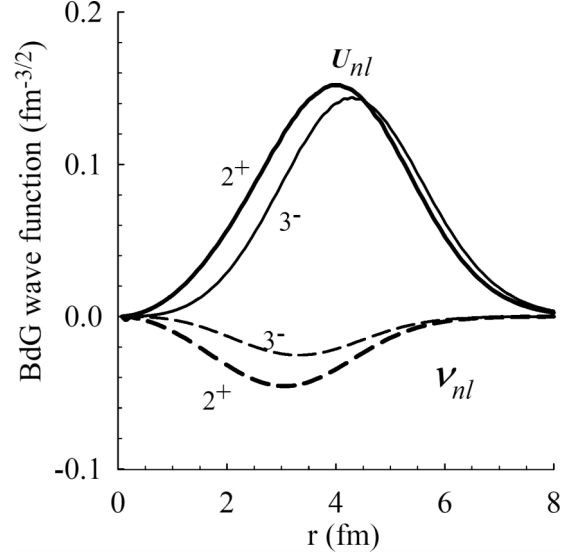
state is considered to be a predisposition that causes the macroscopic wave nature aspect, the condensation aspect of the duality, of the α cluster states in the excited energy region.

In Fig. 5 the BdG wave functions $\mathcal{U}_{n\ell}(r)$ and $\mathcal{V}_{n\ell}(r)$ of Eq. (21) for the 2^+ and 3^- states are displayed. The peak of $\mathcal{U}_{n\ell}(r)$ for $\ell \neq 0$ is located in the surface region because of the repulsive force between the α clusters and moves outward with increasing ℓ due to the centrifugal force. The magnitude of $\mathcal{V}_{n\ell}(r)$ is negligible for the 2^+ and 3^- states, implying no Bogoliubov mixing in these states due to the small condensation rate. As for the zero-mode wave function, I introduce the eigenstate of $\hat{Q}$, denoted by $|q\rangle$, as $\hat{Q}|q\rangle = q|q\rangle$. To solve Eq. (26), I move to the q-diagonal representation, in which the state is represented by the wave function $\Psi_\nu(q) = \langle q|\Psi_\nu\rangle$, and the operators $\hat{Q}$ and $\hat{P}$ are represented by q and $\frac{1}{i}\frac{\partial}{\partial q}$, respectively, consistent with the commutation relation, $[\hat{Q}, \hat{P}] = i$. In Fig. 6 the zero-mode wave functions $\Psi_\nu(q)$ for the first three states obtained by solving Eq. (26) are displayed. Figure 6(a) corresponds to the ground state with $\nu = 0$ and Fig. 6(b) corresponds to the second state with $\nu = 1$, the mysterious 0^+ state at 3.35 MeV. Figure 6(c) corresponds to the third member state with $\nu = 2$, 0_4^+ at 7.30 MeV. One sees that the excitation of the NG mode is caused by the nodal excitation of $\Psi_\nu(q)$ with respect to q in the NG subspace. It is important to note that this nodal excitation is anharmonic, as seen in $\hat{H}_u^{QP}$ in Eq. (24), which brings the excitation energy of the $\nu = 1$ state lower and closer to the vacuum, and the $\nu = 2$ state closer to the $\nu = 1$ state in Fig. 3. The importance of the zero-mode in the BEC systems of α clusters is discussed in detail in Ref. [69].

V. DISCUSSION

I study the condensation rate dependence of the calculated energy levels. In Fig. 7 the energy levels calculated for
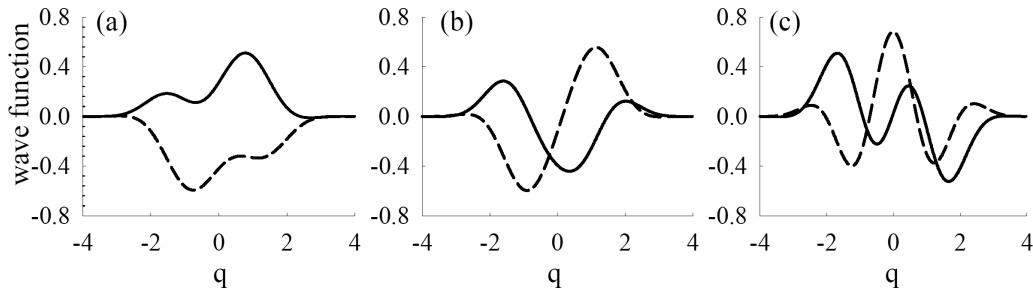
FIG. 6. The zero-mode wave functions $\Psi_\nu(q)$ for the 0^+ states of ^{40}Ca calculated with the condensation rate 6%, $N_0 = 0.06N$, (a) $\nu = 0$, (b) $\nu = 1$, and (c) $\nu = 2$. The solid lines and the dashed lines represent the real part and the imaginary part of the wave functions $\Psi_\nu(q)$.

different condensation rates, 5%, 6%, 7%, and 8%, are displayed. The confining potential parameter Ω and the repulsive potential V_r are slightly adjusted in order to prevent the system from collapsing and the excitation energy of first excited 0^+ state corresponds to the experimental energy: $\Omega = 3.14$ MeV/$\hbar$ and $V_r = 696$ MeV for 5%, $\Omega = 2.99$ MeV/$\hbar$ and $V_r = 555$ MeV for 7%, and $\Omega = 3.04$ MeV/$\hbar$ and $V_r = 535$ MeV for 8%. As the condensation decreases, the repulsive potential becomes larger gradually to keep the system stable, preventing collapse, while the values of Ω change little since they are related to the size of the ground state. As seen in Fig. 7, the structure of the energy spectrum changes generally little. In detail, the excitation energies of the 0_2^+, 2^+, 4^+, 3^-, and 1^- states scarcely change for the different condensation rates. However, for the 0^+ states, the excitation energy of the zero-mode $\nu = 2$ state decreases as the condensation rate increases gradually: In the case of 5% the excitation energy of the $\nu = 2$ zero-mode state, 10.49 MeV, is higher than the BdG 0^+ state. In the case of 6% the $\nu = 2$ zero-mode state comes down to 7.51 MeV. For 8% the $\nu = 2$ zero-mode 0^+ state becomes lower than the BdG 0^+ state. In the range of 6%–8% the calculated 0^+ states correspond to the experimental energy spectrum.
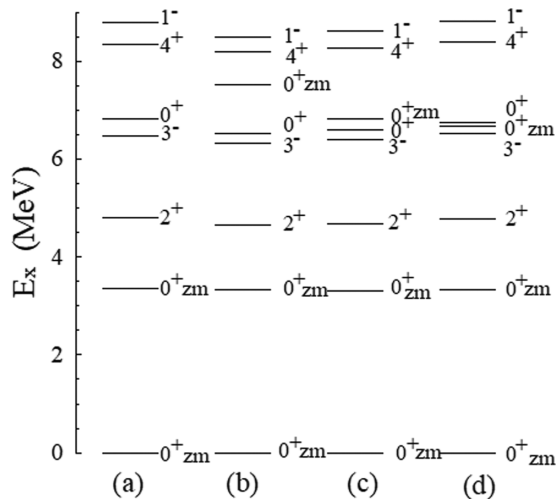
Next I consider the crystallinity and the condensation aspects of the duality of the α cluster structure by comparing the energy levels calculated by using the OCM with the $\alpha + {}^{36}$Ar cluster model in Ref. [88] and those by using the SCM. In Fig. 8, both models reproduce the very low-lying mysterious 0^+ state in agreement with experiment. While the OCM describes the mysterious 0^+ state as a deformed state with the $\alpha + {}^{36}$Ar geometrical configuration, which is in line with the 4p-4h dominant state in the deformed shell model picture of Gerace and Green [71], the SCM describes it as a Nambu-Goldstone zero-mode state, a soft mode. In the crystallinity picture, the mysteriously low excitation energy is brought about by the energy gain due to deformation caused by the geometrical α clustering. This mechanism is common to the deformed shell model by Gerace and Green in Ref. [71], in which the deformation is not due to crystallinity but due to the deformation of the mean field of the shell model. It is to be noted that the observed significant α spectroscopic factor of the mysterious 0^+ state, $S_\alpha^2 = 0.26$, is explained by taking into account the deformation due to α clustering [88]. In the OCM the predisposition of α clustering is implemented in the ground state vacuum. In fact, the calculated ground state has the α spectroscopic factors $S_\alpha^2 = 0.086$ for
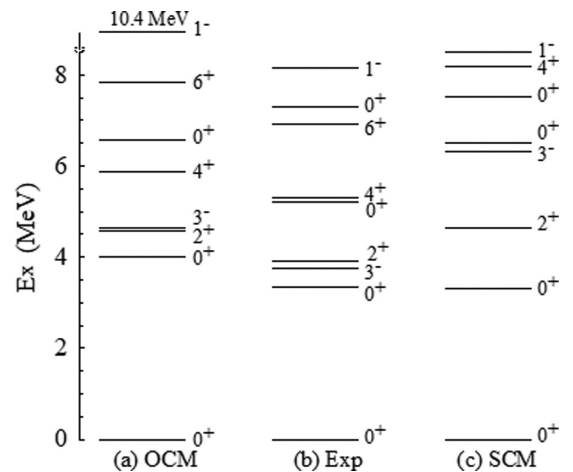

FIG. 7. The condensation rate dependence of the energy levels of ^{40}Ca calculated by the superfluid cluster model with the condensation rates (a) 5%, (b) 6%, (c) 7%, and (d) 8%. The three zero-mode states with $\nu = 0$, 1, and 2 are indicated by zm and others are BdG states.

FIG. 8. (a) The energy levels calculated with the α cluster model with the $\alpha + {}^{36}$Ar geometrical configuration in the OCM [88] are compared with (b) the experimental energy levels [93] and (c) the field theoretical superfluid cluster model calculation with 6% condensation rate assuming no geometrical configuration.

the $(I \otimes L) = (0 \otimes 0)$ channel with the $[{}^{36}\text{Ar}(I) \otimes \alpha_L]_{J=0}$ configuration, where L is the orbital angular momentum of the relative motion between ${}^{36}\text{Ar}$ and α clusters in ${}^{40}\text{Ca}$. On the other hand, in the SCM the emergence of the mysterious low excitation energy 0^+ state is a manifestation of the emergence of a soft mode due to spontaneous symmetry breaking of the global phase of the ground state, condensation aspect of the duality.

The moment of inertia of the $K = 0^+$ band calculated in the OCM is in agreement with the experimental value, while that of the SCM is slightly smaller than that in the OCM calculation. The SCM locates the 2^+ and 4^+ states at excitation energies higher than the experiment. However, while OCM describes the band as a rotational band of the geometrical $\alpha + {}^{36}\text{Ar}$ cluster structure, the SCM gives the band as the BdG states. Although the two models, two views, are completely different, they both basically describe the α cluster structure aspects of the $K = 0^+$ band of ${}^{40}\text{Ca}$.

As for the other excited 0^+ states with the α cluster structure above $E_x = 5$ MeV, the OCM calculation locates only one 0^+ state between 5 and 8 MeV, which has the configuration $[{}^{36}\text{Ar}(2^+) \otimes \alpha_{L=2}]_{J=0}$. More 0^+ states will be obtained in the extended $\alpha + \alpha + {}^{36}\text{Ar}$ cluster model, since the existence of a 0^+ state with 8p-8h character has been suggested in the deformed model and shell model calculations in Refs. [72,73] and in the ${}^{8}\text{Be}$ transfer reaction experiment in Ref. [94]. The SCM locates the two α cluster 0^+ states in the relevant energy region; one is a zero-mode state and the other is a BdG state.

As for the negative parity states, the OCM locates the 1^- state of the $K = 0^-$ band with the $\alpha + {}^{36}\text{Ar}$ structure, which is the parity-doublet partner of the $K = 0^+$ band. As seen in Fig. 8, its calculated excitation is slightly higher than the observed state. On the other hand, the SCM locates the 1^- state as a BdG state, whose excitation energy is in good agreement with the experiment. As for the 3^- state, the OCM locates a low-lying 3^- state, which is a superposition of many channels with the $[{}^{36}\text{Ar}(I) \otimes \alpha_L]_{J=3}$ configuration with the components, 0.047, 0.055, 0.037, 0.063, 0.047, 0.036. 0.034, and 0.071 for the channels $(I \otimes L) = (0 \otimes 3)$, $(2 \otimes 1)$, $(2 \otimes 3)$, $(2 \otimes 5)$, $(4 \otimes 1)$, $(4 \otimes 3)$, $(4 \otimes 5)$, and $(4 \otimes 7)$, respectively. On the other hand, the SCM calculation locates the first 3^- as a BdG state at an excitation energy slightly higher than the experiment. The two results seem to be consistent that this 3^- state has a vibrational character.

Considering that the SCM describes the α clustering aspects in view of wave nature, the α cluster structure in ${}^{40}\text{Ca}$ is found to be understood from both the viewpoints of crystallinity and condensation associated with superfluidity, a property of supersolidity. It is found in the SCM that the emergence of the 0^+ state at very low excitation energy, which is mysterious from the viewpoint of multiparticle multihole excitation in the shell model, is the consequence of the first excited 0^+ being a collective state with a soft mode nature caused by the NG zero mode due to the spontaneous symmetry breaking of the vacuum ground state due to the condensation aspect, superfluidity, of the duality of α clustering. This mechanism is quite general when SSB of the global phase of the vacuum occurs. In the previous paper [17] the mysterious 0^+ state in ${}^{12}\text{C}$, the Hoyle state, was understood

as a soft mode state of the zero mode due to SSB due to the condensation aspect of the duality of α cluster structure of the vacuum ground state.

What is the evidence for the supersolidity? The direct evidence of supersolidity is the observation of a Nambu-Goldstone mode [14–16] due to SSB of the global phase, as was confirmed very recently for an optical lattice supersolid [11–13]. Since the superfluid density ρ_s is the order parameter of the SSB of the global phase [17], the existence of $\rho_s \neq 0$ in the GCM α cluster wave function of the ground state due to the duality accompanies a Nambu-Goldstone mode state, which is a very low-lying collective state and is difficult to explain in the shell model. This logic is same as the emergence of rotational band states in deformed nuclei. Quadrupole deformation with the order parameter $\delta \neq 0$ is caused by a quadrupole boson condensation in the ground state due to SSB of rotational invariance [27]. The appearance of the intruder collective states at a very low excitation energy near the α threshold such as the mysterious 0_2^+ states in ${}^{40}\text{Ca}$ and in ${}^{16}\text{O}$, analogous to the intruder 0_2^+ state in ${}^{12}\text{C}$, which has been understood by the empirical threshold rule of the Ikeda diagram [47,55], is considered to be understood from the viewpoint of the Nambu-Goldstone mode due to SSB of the global phase of the α cluster structure.

It is to be noted that the present reasonable success of the SCM, which assumes no geometrical α cluster configuration, does not mean ruling out the geometrical α cluster model. It should be emphasized that the SCM only describes the condensation, superfluid, aspect of the duality of the α cluster structure, being complementary to the geometrical α cluster picture. In the α cluster structure the geometrical structure is essential. The SCM does not replace the geometrical α cluster model. For example, the rotation motion, the large moment of inertia, is caused by the spontaneous symmetry breaking of the rotational invariance due to the geometrical α cluster configuration, which is absent in the present SCM under a spherical trapping potential. The reduction of the moment of inertia in the SCM calculations is inherent to superfluidity, which is well known in the superfluid heavy nuclei [27]. A cluster model with a geometrical configuration which involves the order parameter to characterize the condensation of α clusters is a future work to be studied.

Finally I mention the importance of the Pauli principle for the duality of geometrical crystallinity and condensation of α cluster structure. The geometrical crystallinity of the α clusters has been known to be caused by the Pauli principle [41,95]. In Figs. 1(c), 1(f), 1(i), and 1(l) of each nucleus the coherent wave of the α cluster structure is the consequence of the geometrical crystallinity. Thus the Pauli principle has the dual role of causing the geometrical clustering and condensation. In this sense the origin of the superfluidity of α cluster structure is different from that of the BCS superfluidity in heavy nuclei and cold atoms.

VI. SUMMARY

It was shown that the spatially localized Brink α cluster model in the generator coordinate method has the apparently incompatible duality of crystallinity and condensation of α

clusters, a property of a supersolid. In order to see whether the α cluster structure, which in recent decades has been understood based on the crystallinity picture with a geometrical configuration of clusters, is also understood from the other aspect of the duality, condensation, a field theoretical cluster model is used in which the order parameter of condensation is introduced. The α cluster structure of ^{40}Ca with a mysterious 0^+ state at very low excitation energy was investigated by the SCM with ten α clusters. Since the SCM rigorously treats spontaneous symmetry breaking of the global phase, a Nambu-Goldstone collective mode, zero mode, due to condensation inevitable appears. It is shown that the mysterious 0^+ state, which is considered to be a bandhead state of the $K = 0^+$ band with the $\alpha + ^{36}$Ar cluster structure in the crystallinity picture, is understood as an NG zero-mode state. The 1^- state, which is considered in the crystallinity picture to be a bandhead state of the $K = 0^-$ band, which is a parity-doublet partner of the $K = 0^+$ band, is obtained as a BdG state in correspondence to the experimental data. The two α cluster 0^+ states at around 6 MeV are also obtained in accordance with the experimental data. Thus it is found that the low-lying α cluster states, which have been considered to be understood in the geometrical cluster picture, can be also understood from the other aspect of the duality, condensation. The mysterious 0^+ state of ^{40}Ca is a collective mode, a soft mode, of the NG mode caused by SSB of the ground state vacuum. This explains naturally why the mysterious low-lying 0^+ state appears below or near the α threshold energy of ^{40}Ca. This mechanism is logically the same as the emergence of the NG mode rotational band states in deformed nuclei, which is caused by a quadrupole boson condensation due to SSB of rotational invariance [27]. The appearance of such intruder collective states near the α threshold, which has been understood by the empirical threshold rule of the Ikeda diagram [47,55], is understood to be due to the NG mode state due to condensation of the α cluster structure. The dual property of crystallinity and condensation, a property of a supersolid, of α cluster structure may be a general feature of the α cluster structure. Since the Pauli principle is responsible for clustering [41,95], one can say that supersolidity of α cluster structure is the consequence of the Pauli principle.

[1] A. F. Andreev and I. M. Lifshitz, Zh. Eksp. Teor. Fiz. **56**, 2057 (1969)[JETP **29**, 1107 (1969)].

[2] G. V. Chester, Phys. Rev. A **2**, 256 (1970).

[3] A. J. Leggett, Phys. Rev. Lett. **25**, 1543 (1970).

[4] H. Matsuda and T. Tsuneto, Prog. Theor. Phys. Suppl. **46**, 411 (1970).

[5] M. Boninsegni and N. V. Prokof'ev, Rev. Mod. Phys. **84**, 759 (2012).

[6] J. Léonard, A. Morales, P. Zupancic, T. Esslinger, and T. Donner, Nature (London) **543**, 87 (2017).

[7] J.-R. Li, J. Lee, W. Huang, S. Burchesky, B. Shteynas, F. C. Top, A. O. Jamison, and W. Ketterle, Nature (London) **543**, 91 (2017).

[8] L. Tanzi, E. Lucioni, F. Famà, J. Catani, A. Fioretti, C. Gabbanini, R. N. Bisset, L. Santos, and G. Modugno, Phys. Rev. Lett. **122**, 130405 (2019).

[9] F. Böttcher, J.-N. Schmidt, M. Wenzel, J. Hertkorn, M. Guo, T. Langen, and T. Pfau, Phys. Rev. X **9**, 011051 (2019).

[10] L. Chomaz, D. Petter, P. Ilzhöfer, G. Natale, A. Trautmann, C. Politi, G. Durastante, R. M. W. van Bijnen, A. Patscheider, M. Sohmen, M. J. Mark, and F. Ferlaino, Phys. Rev. X **9**, 021012 (2019).

[11] L. Tanzi, S. M. Roccuzzo, E. Lucioni, F. Famà, A. Fioretti, C. Gabbanini, G. Modugno, A. Recati, and S. Stringari, Nature (London) **574**, 382 (2019).

[12] G. Natale, R. M. W. van Bijnen, A. Patscheider, D. Petter, M. J. Mark, L. Chomaz, and F. Ferlaino, Phys. Rev. Lett. **123**, 050402 (2019).

[13] M. Guo, F. Böttcher, J. Hertkorn, J.-N. Schmidt, M. Wenzel, H. P. Büchler, T. Langen, and T. Pfau, Nature (London) **574**, 386 (2019).

[14] Y. Nambu, Phys. Rev. **117**, 648 (1960).

[15] J. Goldstone, Nuovo Cimento **19**, 154 (1961).

[16] Y. Nambu and G. Jona-Lasinio, Phys. Rev. **122**, 345 (1961).

[17] S. Ohkubo, J. Takahashi, and Y. Yamanaka, Prog. Theor. Exp. Phys. **2020**, 041D01 (2020).

[18] W. Wefelmeier, Z. Phys. **107**, 332 (1937).

[19] J. A. Wheeler, Phys. Rev. **52**, 1083 (1937).

[20] J. A. Wheeler, Phys. Rev. **52**, 1107 (1937).

[21] J. M. Blatt and V. F. Weisskopf, *Theoretical Nuclear Physics* (Wiley, New York, 1952).

[22] M. G. Mayer, Phys. Rev. **75**, 1969 (1949).

[23] O. Haxel, J. H. D. Jensen, and H. E. Suess, Phys. Rev. **75**, 1766 (1949).

[24] A. Bohr, Kgl. Dan. Mat-Fys. Medd. **26**, 14 (1952).

[25] A. Bohr and B. R. Mottelson, *Nuclear Structure* (W. A. Benjamin, New York, 1969), Vol. I.

[26] A. Bohr and B. R. Mottelson, *Nuclear Structure* (W. A. Benjamin, New York, 1969), Vol. II.

[27] P. Ring and P. Schuck, *The Nuclear Many-Body Problem* (Springer-Verlag, Berlin, 1980).

[28] A. Arima, H. Horiuchi, and T. Sebe, Phys. Lett. B **24**, 129 (1967).

[29] T. Marumori and K. Suzuki, Nucl. Phys. A **106**, 610 (1968).

[30] K. Ikeda, T. Marumori, R. Tamagaki, and H. Tanaka, Prog. Theor. Phys. Suppl. **52**, 1 (1972), and references therein.

[31] K. Wildermuth and Y. C. Tang, *A Unified Theory of the Nucleus* (Vieweg, Braunschweig, 1977).

[32] K. Ikeda, H. Horiuchi, and S. Saito, Prog. Theor. Phys. Suppl. **68**, 1 (1980), and references therein.

[33] S. Ohkubo, M. Fujiwara, and P. E. Hodgson, Prog. Theor. Phys. Suppl. **132**, 1 (1998), and references therein.

[34] S. Ohkubo, T. Yamaya, and P. E. Hodgson, Nuclear clusters, in *Nucleon-Hadron Many-Body Systems*, edited by H. Ejiri and H. Toki (Oxford University Press, Oxford, 1999), p. 150.

[35] D. Brink, in *Proceedings of the International School of Physics "Enrico Fermi"*, Many Body Description of Nuclear Structure and Reactions, Course XXXVI, edited by C. Bloch (Academic, London, 1966), p. 247.

[36] H. Horiuchi, Prog. Theor. Phys. Suppl. **62**, 90 (1977).

[37] S. Saito, Prog. Theor. Phys. **41**, 705 (1969).

[38] B. Buck, C. B. Dover, and J. P. Vary, Phys. Rev. C **11**, 1803 (1975).

[39] S. Ohkubo, Y. Kondo, and S. Nagata, Prog. Theor. Phys. **57**, 82 (1977).

[40] F. Michel, J. Albinski, P. Belery, Th. Delbar, Gh. Grégoire, B. Tasiaux, and G. Reidemeister, Phys. Rev. C **28**, 1904 (1983).

[41] S. Ohkubo, Phys. Rev. C **93**, 041303(R) (2016).

[42] H. Horiuchi, Prog. Theor. Phys. **43**, 375 (1970).

[43] J. Hiura and R. Tamagaki, Prog. Theor. Phys. Suppl. **52**, 25 (1972), and references therein.

[44] E. Uegaki, S. Okabe, Y. Abe, and H. Tanaka, Prog. Theor. Phys. **57**, 1262 (1977).

[45] E. Uegaki, Y. Abe, S. Okabe, and H. Tanaka, Prog. Theor. Phys. **62**, 1621 (1979).

[46] Y. Fukushima and M. Kamimura, J. Phys. Soc. Jpn. **44**, 225 (1978).

[47] H. Horiuchi, K. Ikeda, and Y. Suzuki, Prog. Theor. Phys. Suppl. **52**, 89 (1972).

[48] J. Hiura, F. Nemoto, and H. Bando, Prog. Theor. Phys. Suppl. **52**, 173 (1972).

[49] Y. Fujiwara, H. Horiuchi, K. Ikeda, M. Kamimura, K. Kato, Y. Suzuki, and E. Uegaki, Prog. Theor. Phys. Suppl. **68**, 29 (1980).

[50] F. Michel, S. Ohkubo, and G. Reidemeister, Prog. Theor. Phys. Suppl. **132**, 7 (1998).

[51] S. Elhatisari, N. Li, A. Rokash, J. M. Alarcón, D. Du, N. Klein, *et al.*, Phys. Rev. Lett. **117**, 132501 (2016).

[52] J.-P. Ebran, M. Girod, E. Khan, R. D. Lasseri, and P. Schuck, Phys. Rev. C **102**, 014305 (2020).

[53] A. Tohsaki, H. Horiuchi, P. Schuck, and G. Röpke, Phys. Rev. Lett. **87**, 192501 (2001).

[54] B. Zhou, Y. Funaki, H. Horiuchi, and A. Tohsaki, Front. Phys. **15**, 14401 (2020).

[55] K. Ikeda, N. Takigawa, and H. Horiuchi, Prog. Theor. Phys. Suppl. **E68**, 464 (1968).

[56] R. Tamagaki, Prog. Theor. Phys. Suppl. **E68**, 242 (1968).

[57] D. M. Dennison, Phys. Rev. **96**, 378 (1954).

[58] R. Bijker and F. Iachello, Phys. Rev. Lett. **112**, 152501 (2014).

[59] C. J. Halcrow, C. King, and N. S. Manton, Phys. Rev. C **95**, 031303(R) (2017).

[60] C. J. Halcrow, C. King, and N. S. Manton, Int. J. Mod. Phys. E **28**, 1950026 (2019).

[61] C. J. Halcrow and J. I. Rawlinson, Phys. Rev. C **102**, 014314 (2020).

[62] M. Bouten, Nuovo Cimento **26**, 63 (1962).

[63] D. M. Brink and A. Weiguny, Nucl. Phys. A **120**, 59 (1968).

[64] D. M. Brink, H. Friedrich, A. Weiguny, and C. W. Wong, Phys. Lett. B **33**, 143 (1970).

[65] F. Nemoto, Y. Yamamoto, H. Horiuchi, Y. Suzuki, and K. Ikeda, Prog. Theor. Phys. **54**, 104 (1975).

[66] R. Bijker and F. Iachello, Nucl. Phys. A **1006**, 122077 (2021).

[67] Y. Nakamura, J. Takahashi, Y. Yamanaka, and S. Ohkubo, Phys. Rev. C **94**, 014314 (2016).

[68] Y. Nakamura, J. Takahashi, Y. Yamanaka, and S. Ohkubo, Phys. Rev. C **98**, 049901(E) (2018).

[69] R. Katsuragi, Y. Kazama, J. Takahashi, Y. Nakamura, Y. Yamanaka, and S. Ohkubo, Phys. Rev. C **98**, 044303 (2018), and references therein.

[70] G. E. Brown and A. M. Green, Nucl. Phys. **75**, 401 (1966).

[71] W. J. Gerace and A. M. Green, Nucl. Phys. A **93**, 110 (1967).

[72] W. J. Gerace and A. M. Green, Nucl. Phys. A **123**, 241 (1969).

[73] M. Sakakura, A. Arima, and T. Sebe, Phys. Lett. B **61**, 335 (1976).

[74] K. Takada and S. Tazaki, Prog. Theor. Phys. **52**, 1205 (1974).

[75] M. Hasegawa, Prog. Theor. Phys. **60**, 309 (1978).

[76] J.-P. Ebran, E. Khan, T. Nikšić, and D. Vretenar, Phys. Rev. C **90**, 054329 (2014).

[77] M. Chernykh, H. Feldmeier, T. Neff, P. von Neumann-Cosel, and A. Richter, Phys. Rev. Lett. **98**, 032501 (2007).

[78] Y. Taniguchi, Prog. Theor. Exp. Phys. **2014**, 73D01.

[79] N. Furutachi *et al.*, Prog. Theor. Phys. **119**, 403 (2008).

[80] M. Włoch, D. J. Dean, J. R. Gour, M. Hjorth-Jensen, K. Kowalski, T. Papenbrock, and P. Piecuch, Phys. Rev. Lett. **94**, 212501 (2005).

[81] T. Ogawa, Y. Suzuki, and K. Ikeda, Prog. Theor. Phys. **57**, 1072 (1977).

[82] Y. Suzuki, Prog. Theor. Phys. **55**, 1751 (1976).

[83] Y. Suzuki, Prog. Theor. Phys. **56**, 111 (1976).

[84] S. Ohkubo and K. Umehara, Prog. Theor. Phys. **80**, 598 (1988).

[85] T. Yamaya, M. Saito, M. Fujiwara, T. Itahashi, K. Katori, T. Suehiro, S. Kato, S. Hatori, and S. Ohkubo, Phys. Lett. B **306**, 1 (1993).

[86] T. Yamaya, K. Katori, M. Fujiwara, S. Kato, and S. Ohkubo, Prog. Theor. Phys. Suppl. **132**, 73 (1998).

[87] T. Yamaya, M. Saitoh, M. Fujiwara, T. Itahashi, K. Katori, T. Suehiro, S. Kato, S. Hatori, and S. Ohkubo, Nucl. Phys. A **573**, 154 (1994).

[88] T. Sakuda and S. Ohkubo, Phys. Rev. C **49**, 149 (1994).

[89] T. Sakuda and S. Ohkubo, Prog. Theor. Phys. Suppl. **132**, 103 (1998).

[90] N. S. Manton, Int. J. Mod. Phys. E **29**, 2050018 (2020).

[91] J. Takahashi, Y. Yamanaka, and S. Ohkubo, Prog. Theor. Exp. Phys. **2020**, 093D03.

[92] S. Ali and A. R. Bodmer, Nucl. Phys. **80**, 99 (1966).

[93] F. Ajzenberg-Selove, Nucl. Phys. A **506**, 1 (1990); Brookhaven National Laboratory, National Nuclear Data Center, http://www.nndc.bnl.gov/ensdf/

[94] R. Middleton, J. D. Garrett, and H. T. Fortune, Phys. Lett. B **39**, 339 (1972).

[95] R. Tamagaki, Prog. Theor. Phys. **42**, 748 (1969).